P1.2 URBAN APPLICATION OF AN ALTERNATIVE FLUX ESTIMATION METHOD

Christopher A. Biltoft
Adiabat Meteorological Services, Salt Lake City, Utah

Eric R. Pardyjak
Department of Mechanical Engineering, University of Utah
Salt Lake City, Utah

1. INTRODUCTION

An adequate depiction of Reynolds stress tensor ($\boldsymbol{\tau}$) components, particularly the turbulent vertical flux of horizontal momentum, is necessary to achieve an understanding of flow within an urban boundary layer (UBL). Stress components are typically obtained through eddy correlation of measurements made using a tri-axis sonic anemometer-thermometer(sonic). Sonics can provide the collocated measurements needed to compute longitudinal (u), lateral (v), and vertical (w) velocities over a range of temporal and spatial scales that is usually adequate to describe turbulent fluxes within the UBL.

The vertical flux of the longitudinal momentum (u) is a time-average (from $t = t_i$ to $t = t_i + \Delta t$) of individual products of simultaneous w and u measurements represented as $\frac{1}{\Delta t}\int w_i(t)u_i(t)dt$. For uniformly spaced data and Reynolds decomposition this integral reduces to

$$\tau_{wu}/\rho = \Sigma(w_i u_i)/n = \overline{w'u'} + \overline{w}\,\overline{u}, \quad (1)$$

where ρ is density, the subscript i signifies the ith of n measurements at a fixed point, Σ indicates summation from the first to the nth measurement, the overbar signifies a temporal average, and primed quantities represent differences of individual measurements from that time average ($u_i' = u_i - \overline{u}$). Means of individual primed quantities are zero, and the mean vertical velocity $\overline{w}$ is either assumed to be zero, coordinate rotations force it to zero, or $\overline{w}\,\overline{u}$ is left as a residual. Our focus is on the turbulent vertical momentum flux, $\overline{w'u'}$, where the first term (w') is acting on u'.

When the velocity components are aligned with the mean wind in a Cartesian coordinate frame, $\boldsymbol{\tau}$ components can be represented as products of velocity fluctuations:

$$\boldsymbol{\tau} = \begin{bmatrix} \tau_{xx} & \tau_{xy} & \tau_{xz} \\ \tau_{yx} & \tau_{yy} & \tau_{yz} \\ \tau_{zx} & \tau_{zy} & \tau_{zz} \end{bmatrix} =$$

Corresponding author address: Christopher A. Biltoft, 674 16th Avenue, Salt Lake City, UT 84103, biltoftc@yahoo.com

$$-\rho \begin{bmatrix} \overline{u'u'} & \overline{u'v'} & \overline{u'w'} \\ \overline{v'u'} & \overline{v'v'} & \overline{v'w'} \\ \overline{w'u'} & \overline{w'v'} & \overline{w'w'} \end{bmatrix}. \quad (2)$$

An urban boundary layer differs from the atmospheric boundary layer over open terrain by the presence of large non-porous obstacles (buildings) and other roughness elements that tend to dampen larger scale motions found in the free atmosphere, and increase smaller scale largely incoherent turbulent motions. Flow in an urban street canyon, as discussed by Nakamura and Oke (1988), is constrained by sidewalls, and the primary flow direction is determined by the angle of attack between street orientation and the overlying flow. Turbulence is generated through interaction of this constrained flow with individual roughness elements. Flow near the top of the urban roughness layer rapidly changes angular direction as it passes over or around obstacles.

A sonic in a fixed mount with exposure to an UBL flow is unlikely to be aligned with the mean wind. Therefore, measured wind components nearly always require coordinate rotations to resolve wind components free of cross-axis contamination and to meet Reynolds averaging requirements. Axis misalignments with respect to the mean flow are described as pitch, roll, and yaw. Pitch and roll represent the misalignment of measured *u* and *v* components with respect to the vertical axis, and yaw represents the misalignment of measured *u* and *v* with respect to the mean wind direction. How coordinate rotations are performed is an important data processing consideration.

A yaw rotation (YR) to align the longitudinal wind component into the mean wind direction (with $\bar{v}=0$), is almost always desirable. Whether or not to proceed with pitch and roll rotations for $\bar{v}=\bar{w}=0$, or with a triple rotation, (producing $\bar{v}=\bar{w}=\overline{w'v'}=0$) depends on the circumstances. Wilczak et al. (2001) and Finnigan (2004) describe and analyze the consequences of these rotations, which can introduce substantial errors when pitch and roll angles, and/or $\overline{w'v'}$ are large. Wilczak et al. (2001) also introduce a planar fit algorithm for use on sloping terrain that simultaneously rotates all stress components to a plane where $\bar{w}=\bar{v}=\overline{w'v'}=0$. However, the complexity of urban flow is such that an adequate planar fit often cannot be achieved. Of the available rotations only YR introduces no rotation-induced errors in highly disturbed urban flows. It is used here for comparison with an alternative introduced below.

Once coordinate axis rotations are completed, momentum flux computation methods must be considered. There are two common ways to define density-normalized momentum flux. It can be the Reynolds stress tensor component aligned with the local mean wind,

$$\tau_A = \overline{w'u'}, \quad (3)$$

or the absolute magnitude of the horizontal Reynolds stress vector,

$$|\tau_B| = (\overline{w'u'}^2 + \overline{w'v'}^2)^{0.5}. \quad (4)$$

Note that the $|\tau_B|$ flux direction (sign) is lost in the computation process, and must be assigned by the user.

2. AN ALTERNATIVE METHOD

An alternative rotation and computation method (tilt, or T method) uses the horizontal component of the scalar wind speed instead of u and v components. The horizontal wind component $s = (u^2 + v^2)^{½}$ represents the wind run h in a direction aligned along the mean wind ($\bar{s}$), and is not necessarily normal to the gravity vector. $\bar{w}$ is normal to $\bar{s}$. The coordinate system is now defined in terms of an *h*-*z* axis with wind components *s* and *w*. Wind speed *s* is functionally equivalent to speed measured using an ideal cup anemometer aligned with the mean wind. In this application, *s* is no longer a scalar wind speed, but is now the magnitude of a vector quantity directed along the axis of the mean wind. Turning of the wind along the horizontal axis, which makes no contribution to horizontal momentum, is absent from an *h*-*z* coordinate system.

The *h*-*z* coordinate system requires a tilt of the coordinate axis through mean angle $\bar{\alpha}$ to render $\bar{w}$=0. Velocity component measurements s_m' and w_m', representing respectively the measured horizontal and vertical turbulence components, are tilted through $\bar{\alpha}$. Tilt geometry produces

$$s' = s_m' \cos\bar{\alpha} + w_m' \sin\bar{\alpha}\ , \qquad (5)$$

and

$$w' = w_m' \cos\bar{\alpha} - s_m' \sin\bar{\alpha}\ , \qquad (6)$$

where

$$\bar{\alpha} = \tan^{-1}(2\,\overline{w_m' s_m'}\,/(\overline{s_m'^2} - \overline{w_m'^2}))/2. \qquad (7)$$

The horizontal momentum flux is the product of the rotated components, which after some simplification is

$$\tau_C = \overline{w's'} = \overline{w_m' s_m'}\,(\cos 2\bar{\alpha}) + ½(\sin 2\bar{\alpha}\,(\overline{w_m'^2} - \overline{s_m'^2})). \qquad (8)$$

Expressing the Reynolds stress in *h*-*z* coordinates simplifies it from nine to four components:

$$\boldsymbol{\tau} = \begin{bmatrix} \tau_{hh} & \tau_{hz} \\ \tau_{zh} & \tau_{zz} \end{bmatrix} = -\rho \begin{bmatrix} \overline{s's'} & \overline{s'w'} \\ \overline{w's'} & \overline{w'w'} \end{bmatrix}. \qquad (9)$$

Note that this simplification leaves no off-diagonal stress components to accumulate errors from the tilt to $\bar{w} = 0$.

3. URBAN APPLICATIONS

Sonic data sets used to compare results from the τ_A, $|\tau_B|$, and τ_C methods are from Oklahoma City, as presented in the 2003 Joint Urban (JU03) program (Clawson et al., 2005). This program included tracer gas releases with wind and turbulence measurements. The JU03 database is found at https://ju2003-dpg.dpg.army.mil/.

Tri-axis sonics selected for the present illustration are the METEK USA-1 mounted on the southeast corner of the Sonic Building roof overlooking Park Avenue in downtown Oklahoma City, and an R.M. Young 81000 mounted on a tower within the Park Avenue urban canyon (Figure 2). The METEK sonic (LANL Blue), operated by Los Alamos National Laboratories, was mounted 47.5 m above ground (street) level (AGL) near the corner of Park and Broadway Streets, and provides an example of rooftop-level flow. The Young sonic, operated by Oklahoma University (OU1-5), was mounted at 15.1 m AGL on OU Tower 1. This height, above the height of surrounding vegetation and other smaller roughness elements, is about one third of the depth of the Park Avenue urban street canyon.

Figure 2 presents Park Avenue building heights and sonic locations. Brown et al. (2003) summarize sonic mounting and location information.

Summary statistics for seven paired one-hour block runs of sonic data (36000 data points) from the LANL Blue and OU1-5 locations are presented in Table 1. These data, identified by date/start time, were obtained during the JU03 intensive operating periods (IOPs), which included tracer releases. Run number, for example 9020, identifies measurements from Julian date 190, 2000-2100 hrs UTC. Sample hourly data blocks include one from IOPs 1, 4, 5, 6, and 9, and two from IOP 8. Table 1 also displays integrated flow direction estimates (IFD, defined below), with respect to true north, mean speeds $\bar{s}$ as measured by the sonics, mean vertical velocities $\bar{w}$ prior to tilt rotation, tilt angles used to reduce $\bar{w}$ to zero, turbulence intensities and along-wind variance summaries from both the YR and T methods, and momentum fluxes computed using methods τ_A, $|\tau_B|$, and τ_C.

Defining wind direction in an urban environment is problematic because the measurements at an individual site are affected by local roughness elements. However, reasonable estimates (±10º) of the integrated flow direction can be derived from the tracer gas concentration footprints downwind of the release site. The half-hourly gas concentration footprints along the 1-, 2-, and 4-km arcs (see Clawson et al., 2005) provide a basis for estimating integrated rooftop wind directions, while the tracer footprints from within the Oklahoma City central business district provide flow estimates through the street canyons.

While wind speeds and turbulence intensities at the LANL Blue and OU1-5 sites are roughly comparable, substantial differences in flow directions and momentum fluxes are evident. Flow through Oklahoma City's urban core was channeled through a grid of E-W and N-S streets, while rooftop flow was subject to deflection as it encountered individual buildings. Flow impinging on the LANL Blue sonic is deflected upward, sometimes at steep tilt angles. Note that tilt angles greater than ±30º exceed standard instrument calibration limits, and probably contain instrument-induced errors due to flow distortion and transducer shadowing. LANL Blue sonic tilt angles are typically large for southerly winds, but are smaller for runs 8018 and 9416 due to their larger easterly (100º) or westerly (210º) flow components. This easterly or westerly flow encountered the Sonic Building at a grazing angle rather than being forced up the face of the building. Urban canyon results from the OU1-5 sonic feature smaller $\bar{w}$ and tilt angles than contemporaneous rooftop values.

Table 1 turbulence intensities

$$I_{YR} = [⅓(\overline{u'u'} + \overline{v'v'} + \overline{w'w'})]^{0.5} / \bar{s} \qquad (10)$$

or

$$I_T = [½(\overline{s's'} + \overline{w'w'})]^{0.5} / \bar{s}, \qquad (11)$$

are very large for both the rooftop and urban canyon locations, although somewhat larger on average at the rooftop. The choice of coordinate rotation algorithm or computation method appears to have a minor impact on turbulence intensities or their contributing variances.

However, the choice of rotation algorithm and computation method produced major differences in

momentum flux estimates, as noted in the Table 1 columns τ_A, $|\tau_B|$, τ_{CV} and τ_{CH} . These differences are magnified at large tilt angles. Flow experienced by LANL Blue, as presented in yaw-rotated τ_A coordinates, indicates strong downward momentum flux in the presence of a large upward mean vertical velocity (runs 8018 and 0807 excepted), while the $|\tau_B|$ results provide no flux direction information. In contrast, the tilt-corrected τ_C results can be partitioned into horizontal (τ_{CH}) and vertical (τ_{CV}) components relevant to urban geometry. As shown in Figure 1, the horizontal component is given by

$$\tau_{CH} = \tau_C \sin(\alpha), \qquad (12)$$

and the vertical component is

$$\tau_{CV} = \tau_C \cos(\alpha). \qquad (13)$$

Using these τ_C components for analysis, down-canyon easterly (Run 8018) and westerly (Run 9416) flows produced downward momentum fluxes that penetrated into the canyon at least to the height of the OU Tower 1 Sonic 5 location. In contrast, cross-canyon flows experienced during the rest of the runs generated upward momentum fluxes at the Sonic Building rooftop level with no discernable momentum penetration into the Park Avenue street canyon.

4. COHERENCE ANALYSIS

A limited amount of information is available from summary statistics alone. Exploring the frequency domain adds a new analysis dimension. Within the frequency domain squared spectral coherence (CH) provides frequency-stratified flux detail and offers the possibility of a test for statistical significance. Coherence of time series w

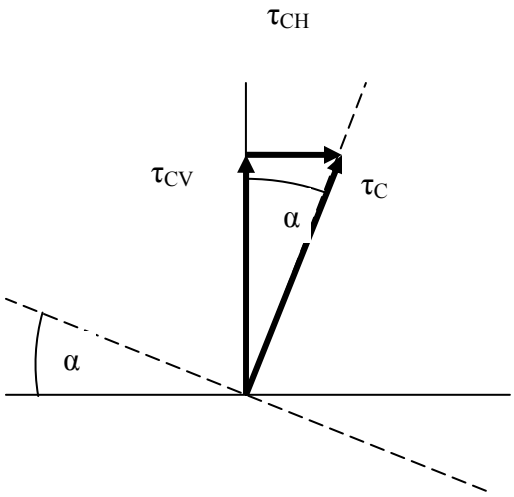

Figure 1. Schematic of tilt through angle α and partition of τ_C into τ_{CH} and τ_{CV} .

and u as used here is the sum of the squared quadrature spectrum (Q^2) plus the squared cospectrum (Co^2) normalized by the geometric time series spectra geometric means, $S_w(f)$ and $S_u(f)$, where f is the normalized frequency band. The squared coherence is defined for *w* and *u* in this context as

$$\mathrm{CH} = \frac{Q^2(f) + Co^2(f)}{S_w(f) S_u(f)}. \qquad (14)$$

Coherence, as presented in (14), varies between 0 and 1, and expresses the degree of linear association between the phases and amplitudes of the two variables within each normalized non-overlapping frequency band, which also ranges from 0 to 1 ($f_j = j/n'$, $j = 0 \ldots n'$). The number of frequency bands is a function of the size of the Fourier transform selected. For a fast Fourier transform of size nfft = 256 used in this analysis the spectrum is divided into nfft/2+1 = 129 frequency bands. The

magnitude of the coherence contribution for each band, unlike the original source data, is independent of the magnitudes of its neighboring frequencies, rendering the coherence results suitable for statistical analysis.

Coherence analysis provides an opportunity to examine the contributions at each normalized frequency band to the total covariance. This is important because fluxes, known to be temporally and spatially intermittent, also vary over scales of motion. Figure 3 displays squared spectral coherence vs. normalized frequency for the LANL Blue rooftop sonic data run 9020. The relative magnitudes and positions of coherence peaks for the yaw-rotated τ_A and tilt-rotated τ_C data sets are evident. (Note that coherence cannot be computed directly for $|\tau_B|$ because it is composed of two sets of covariances.) From Figure 3 it is immediately apparent that the τ_A coherence peaks dominate the lower half of the Figure 3 frequency band, while the τ_C peaks dominate the higher frequencies. This apparent frequency "shift" was commonly observed for in the rooftop data in southerly flow, but was not observed in the urban street canyon, or in along-canyon flow. The low frequency $\overline{w'u'}$ results, associated with the strong downward τ_A flux presented in Table 1, are likely to be a cross-component contamination artifact. The Figure 3 $\overline{w's'}$ peaks, and the associated τ_C in Table 1, better represent the true rooftop turbulent flux. Contrasting urban canyon coherence peaks from OU Tower 1 Sonic 5 (shown in Table 1 and Figure 4) are considerably smaller across the entire frequency band, indicating weak flux in a field of incoherent turbulence.

Following Panofsky and Brier (1965), a spectral coherence significance test was applied to the data sets summarized in Table 1. If a coherence peak at any frequency exceeds a user-defined significance threshold, the coherence and by inference its underlying covariance are considered statistically significant at a user-selected probability level *p*. Panfosky and Brier (1965) provide an approximate formula for estimating *p* thresholds. The size of the Fourier transform (nfft) and sample size *N* appear to contain all of the information needed to define this significance threshold. Given *N*>>nfft, and nfft = 256, the simple relation $\text{nfft}^{0.5}/N^{0.5}$ represents an empirically determined *p* = 2% threshold.

The 2% coherence threshold is represented by a horizontal line across Figures 3 through 6. Multiple coherence peaks extend above the threshold in Figure 3, indicating that the momentum fluxes are statistically significant. For the τ_C case, it is quite likely that these peaks represent both strong upward and downward fluxes that, averaged over a 1-hour data run, nearly cancelled each other. In contrast, coherence peaks shown on Figure 4 all failed to meet the significance threshold, reinforcing the notion of weak fluxes in the urban canyon in the midst of strong incoherent turbulence. Flux peaks that failed to meet the 2% significance threshold are presented in *Italics* in Table 1. This was a predominant condition at night (Runs 0606, 0611, and 0807) in the Park Avenue street canyon.

The Run 9416 coherence results for westerly winds, illustrated in Figures 5 and 6, contrast with those for southerly

winds shown in Figures 3 and 4. Southerly flow produced substantial incoherent turbulence on Park Avenue, but little net momentum exchange. The westerly winds of Run 9416 channeled flow through Park Avenue and produced large low frequency coherence peaks, indicating strong downward momentum flux from rooftop extending through at least mid-canyon levels. Similar effects were observed for easterly flow through Park Avenue.

The right hand column in Table 1 contains the coefficient of correlation (r) between τ_A and τ_C coherence data. The correlation vanishes when tilt angles are large, and is diminished in the absence of a strong coherence peak.

5. CONCLUSIONS

Momentum flux computation within an urban boundary layer is problematic due to effects from local roughness elements. In particular, large tilt angles and lateral turbulence effects make it difficult to compute momentum flux by the usual methods without incurring substantial errors. An alternative approach, which requires computation of wind speed along the mean flow direction, requires only a single coordinate rotation (tilt) to produce a zero mean vertical velocity. Because this method reduces stress tensor components from nine to four, errors generated by lateral wind components are also eliminated. Results from Oklahoma City rooftop and urban canyon locations illustrate the advantages of this momentum flux computation method.

Important flux information becomes available by transforming from the time to frequency domain. In particular, the squared spectral coherence identifies the frequencies at which significant momentum exchange occurs. Southerly winds impinging on the Oklahoma City urban core produced flows with high tilt angles at rooftop levels, with high frequency momentum fluxes that did not penetrate far into the Park Avenue urban canyon. However, easterly or westerly flows oriented down Park Avenue produced substantial low frequency downward momentum fluxes that penetrated well into the urban canyon. The alternative momentum flux estimation method most clearly illustrated these results.

Squared spectral coherence thresholds can be used to determine the statistical significance of flux estimates. Illustrative sample data runs show small, but statistically significant momentum fluxes at a rooftop level. Nocturnal momentum fluxes within the urban street canyon often failed to meet the significance threshold. This coherence threshold test requires further development and testing, but it holds the promise of being a useful covariance analysis tool.

REFERENCES

Brown, M., D. Boswell, G. Streit, M. Nelson, T. McPherson, T. Hilton, E. R. Pardyjak, S. Pol, P. Ramamurthy, B. Hansen, P. Kastner-Klein, J. Clark, A. Moore, D. Walker, N. Felton, D. Strickland, D. Brook, M. Princevac, D. Zajic, R. Wayson, J. MacDonald, G. Fleming, and D. Storwold, 2003: *Joint Urban 2003 Street Canyon Experiment*, AMS Conf. on Urban Zone, Seattle, WA, LA-UR-03-8454, 12 pp.

Clawson, K. L., R. G. Carter, D. J. Lacroix, C. A. Biltoft, N. F. Hukari, R.

C. Johnson, J. D. Rich, S. A. Beard, and T. Strong, 2005: *Joint Urban 2003 (JU03) SF_6 Atmospheric Tracer Field Tests.* NOAA Technical Memorandum OAR ARL-254, Air Resources Laboratory, Silver Spring, Maryland, 216 pp.

Finnigan, J. J., 2004: A Re-Evaluation of Long-Term Flux Measurement Techniques Part II: Coordinate Systems. *Boundary-Layer Meteorol*. **113**, 1-41.

Nakamura, Y., and T. Oke, 1988: Wind, Temperature, and Stability Conditions in an East-West Oriented Canyon. *Atmos. Environ.,* **22,** 2691-2700.

Panofsky, H. A. and G. W. Brier, 1965: *Some Application of Statistics to Meteorology*, The Pennsylvania State University, U.S.A., 224 pp.

Wilczak, J. M., S. P. Oncley, and S.A. Stage, 2001: Sonic Anemometer Tilt Correction Algorithms. *Boundary-Layer Meteorol*., **99**, 127-150.

Table 1. Summary JU03 sonic anemometer data for four daytime (8018, 9020, 9416, and 9716) and three nighttime (0606, 0611, and 0807) data runs each from LANL Sonic Blue and OU Tower 1 Sonic 5. IFD indicates indicated flow direction, and α is the τ_C tilt angle. I_{YR} and I_T are turbulence intensities computed after yaw or tilt rotations. Subscripts YR and T indicate respectively yaw and tilt rotations. τ_{CH} and τ_{CV} are the respective horizontal and vertical components of τ_C.

Run	IFD deg.	$\bar{s}$ ms^{-1}	$\bar{w}$ ms^{-1}	α deg.	I_{YR} (ND)	I_T (ND)	$\overline{u'u'}_{YR}$ m^2s^{-2}	$\overline{s's'}_T$ m^2s^{-2}	$\overline{w'w'}_{YR}$ m^2s^{-2}	$\overline{w'w'}_T$ m^2s^{-2}	τ_A m^2s^{-2}	$\lvert\tau_B\rvert$ m^2s^2	τ_{CV} m^2s^{-2}	τ_{CH} m^2s^2	Peak Coherence		
															τ_A	τ_C	r
LANL Sonic Blue. z = 47.5 m AGL																	
8018	**100**	**3.93**	**0.94**	**14**	**0.32**	**0.32**	**2.882**	**2.502**	**0.725**	**0.653**	**.477**	**.646**	**-.070**	**-.017**	**.456**	**.103**	**.11**
9020	**190**	**2.40**	**1.50**	**38**	**0.61**	**0.57**	**1.589**	**1.470**	**2.210**	**2.449**	**-.396**	**.735**	**.112**	**.087**	**.143**	**.192**	**-.17**
9416	**210**	**1.98**	**0.33**	**10**	**0.41**	**0.44**	**1.042**	**0.811**	**0.572**	**0.694**	**-.327**	**.327**	**-.371**	**-.065**	**.331**	**.254**	**.97**
9716	**190**	**1.80**	**1.23**	**43**	**0.59**	**0.56**	**0.839**	**0.848**	**1.288**	**1.180**	**-.051**	**.395**	**.194**	**.181**	**.159**	**.225**	**-.19**
0606	**160**	**2.85**	**1.70**	**37**	**0.48**	**0.48**	**1.940**	**1.190**	**2.120**	**2.520**	**-.482**	**.697**	**.061**	**.046**	**.191**	**.182**	**-.17**
0611	**170**	**2.68**	**1.56**	**36**	**0.50**	**0.50**	**1.802**	**1.260**	**1.966**	**2.320**	**-.367**	**.565**	**.004**	**.003**	**.188**	**.126**	**-.07**
0807	**180**	**1.90**	**1.30**	**43**	**0.53**	**0.52**	**1.135**	**0.923**	**1.153**	**1.040**	**.088**	**.232**	**.123**	**.115**	**.159**	**.142**	**-.34**
OU Tower 1, Sonic 5, z = 15.1 m AGL																	
8018	**090**	**1.76**	**-0.50**	**16**	**0.43**	**0.42**	**0.704**	**0.681**	**0.492**	**0.437**	**-.070**	**.148**	**-.062**	**-.018**	**.146**	**.123**	**.77**
9020	**210**	**2.81**	**0.08**	**02**	**0.43**	**0.45**	**2.995**	**2.411**	**0.750**	**0.749**	**.105**	**.113**	**-.008**	**-.000**	**.158**	**.140**	**.93**
9416	**260**	**2.16**	**0.22**	**06**	**0.28**	**0.30**	**0.592**	**0.566**	**0.258**	**0.284**	**-.113**	**.113**	**-.140**	**-.015**	**.298**	**.288**	**.92**
9716	**200**	**1.68**	**0.36**	**01**	**0.49**	**0.47**	**1.244**	**0.870**	**0.398**	**0.397**	**.090**	**.107**	**.013**	**.000**	***.076***	**.088**	**.75**
0606	**150**	**1.35**	**-0.12**	**-05**	**0.49**	**0.45**	**0.592**	**0.462**	**0.304**	**0.289**	**.049**	**.079**	**-.073**	**.006**	***.072***	***.065***	**.30**
0611	**160**	**1.32**	**-0.09**	**-04**	**0.50**	**0.46**	**0.634**	**0.480**	**0.252**	**0.244**	**.028**	**.031**	**-.050**	**.003**	***.066***	***.072***	**.37**
0807	**180**	**1.13**	**-0.11**	**-05**	**0.56**	**0.55**	**0.601**	**0.460**	**0.315**	**0.312**	**.001**	**.044**	**-.005**	**.000**	***.075***	***.041***	**.67**

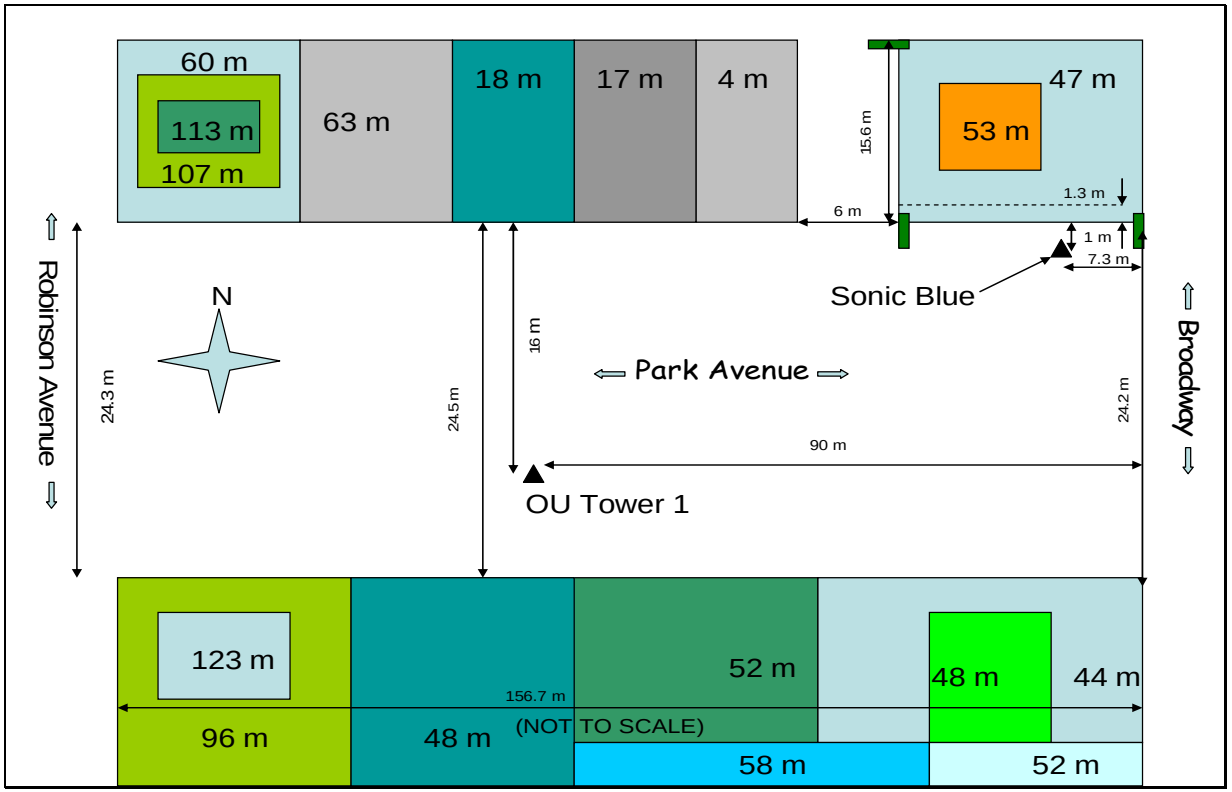

Figure 2. Top-down view of Park Avenue in Oklahoma City, with heights of buildings and locations of LANL Sonic Blue and OU Tower 1 indicated.

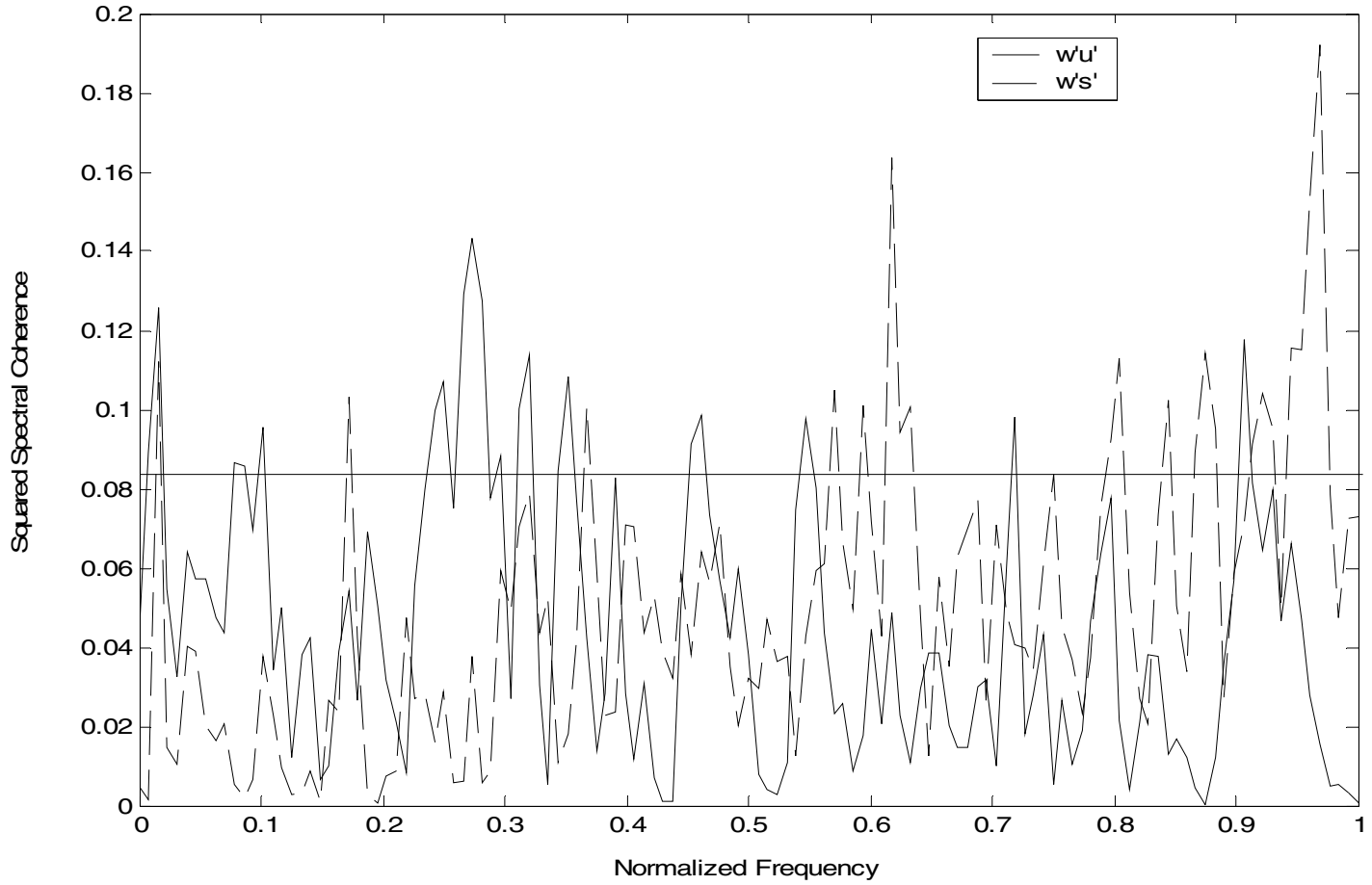

Figure 3. Squared spectral coherence (CH) versus normalized frequency for yaw-rotated $\overline{w'u'}$ and tilt-rotated $\overline{w's'}$ data from the JU03 Oklahoma City experiment (Julian Date 190, 2000-2100 UTC, Run 9020) LANL Sonic Blue mounted on the southeast corner of the Sonic Building at a height of 47.5 m AGL. The 2% significance threshold is indicated by the solid horizontal line at CH = 0.084.

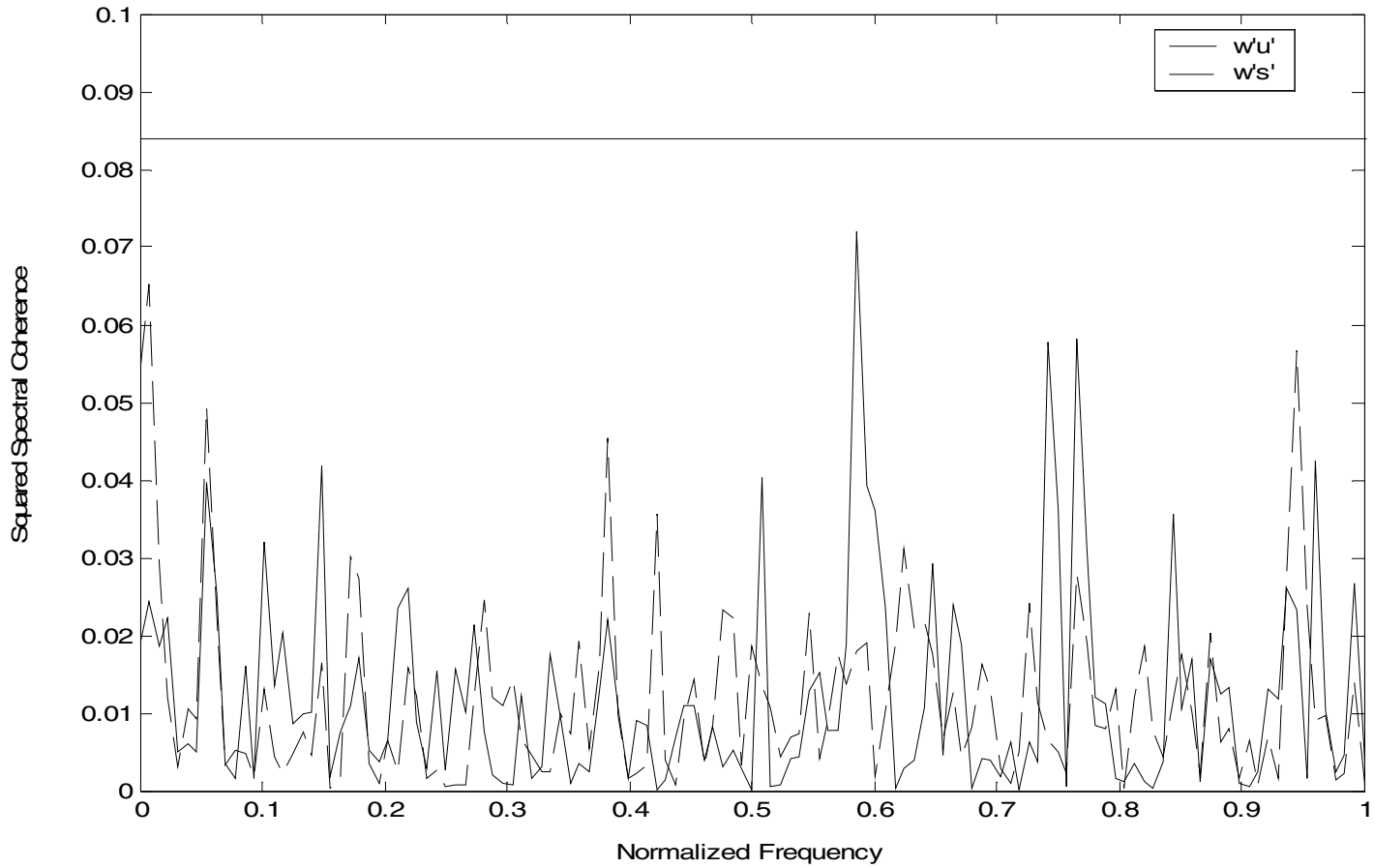

Figure 4. Squared spectral coherence (CH) versus normalized frequency for yaw-rotated $\overline{w'u'}$ and tilt-rotated $\overline{w's'}$ data from the JU03 Oklahoma City experiment (Julian Date 206, 0600-0700 UTC, Run 0606) OU Tower 1 Sonic 5 mounted at 15.1 m AGL within the Park Avenue urban street canyon. The 2% significance threshold is indicated by the solid horizontal line at CH = 0.084.

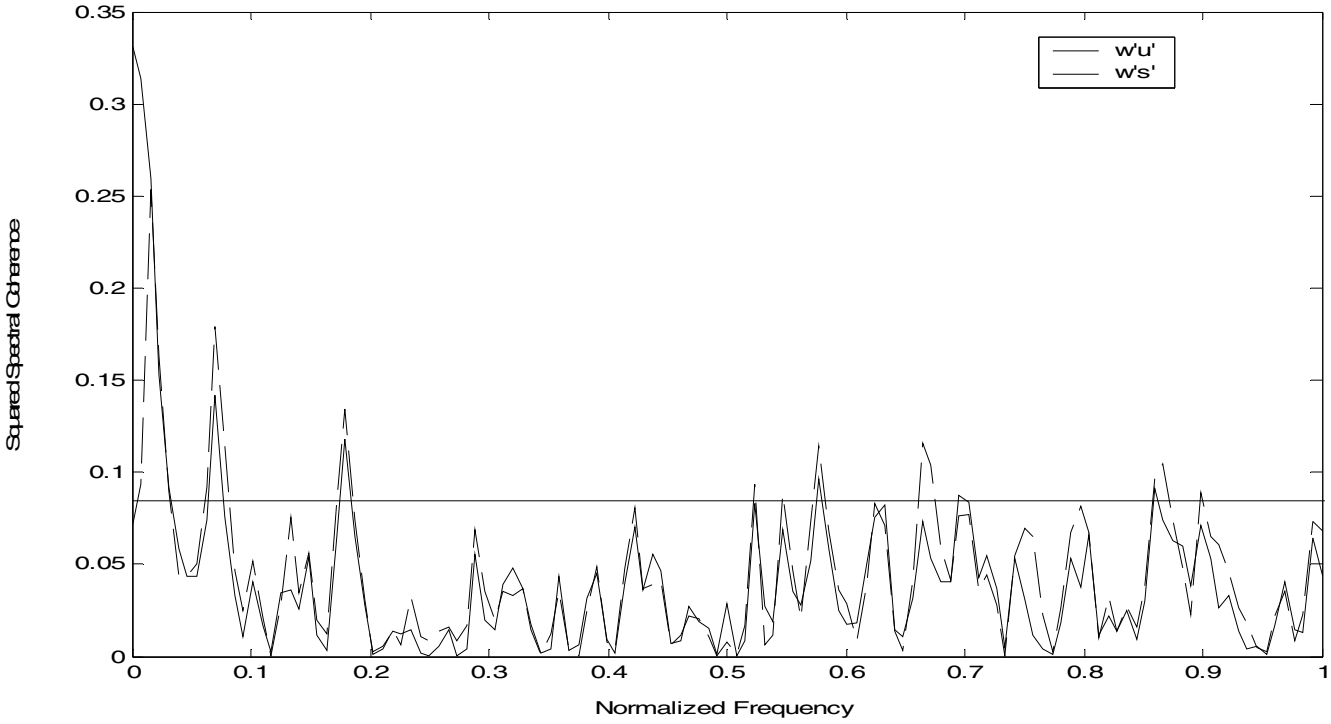

Figure 5. Squared spectral coherence (CH) versus normalized frequency for yaw-rotated $\overline{w'u'}$ and tilt-rotated $\overline{w's'}$ data from the JU03 Oklahoma City experiment (Julian Date 194, 1600-1700 UTC, Run 9416), LANL Sonic Blue mounted on the southeast corner of the Sonic Building at a height of 47.5 m AGL. The 2% significance threshold is indicated by the solid horizontal line at CH = 0.084.

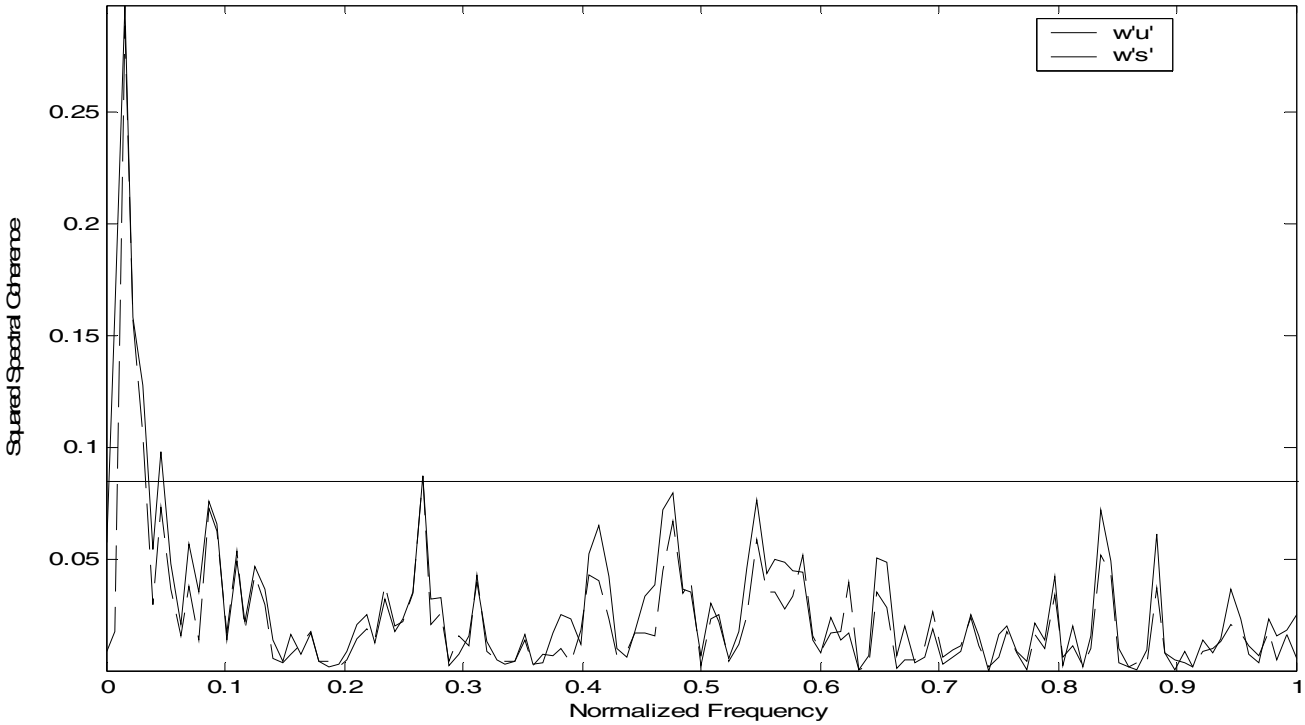

Figure 6. Squared spectral coherence (CH) versus normalized frequency for yaw-rotated $\overline{w'u'}$ and tilt-rotated $\overline{w's'}$ data from the JU03 Oklahoma City experiment (Julian Date 194, 1600-1700 UTC, Run 9416), OU Tower 1 Sonic 5 mounted at 15.1 m AGL within the Park Avenue urban street canyon. The 2% significance threshold is indicated by the solid horizontal line at CH = 0.084.